Design and Applications of a High-Resolution Insert Head-Mounted-Display

Akitoshi Yoshida

Lehrstuhl für Informatik V
Universität Mannheim
68131 Mannheim, GERMANY
+49-621-292-5707
yoshida@mp-sun1.informatik.uni-mannheim.de

Jannick P. Rolland

Department of Computer Science
University of North Carolina at Chapel Hill
Chapel Hill, NC 27599, USA
+1-919-962-1901
rolland@cs.unc.edu

John H. Reif

Department of Computer Science
Duke University
Durham, NC 27708, USA
+1-919-660-6568
reif@cs.duke.edu

Abstract

In this paper, a new Head Mounted Display (HMD) that provides a large field of view with a high-resolution insert is proposed and designed. Previously, this type of HMD has been designed using mechanical or sequential scanning devices, which are bulky and expensive. The proposed High-Resolution Insert HMD (HRI-HMD) is innovative and it uses only electronic devices that can be easily integrated with the optical components. The potential benefit of the HRI-HMD comes not only from its improved visual quality via a high-resolution insert but also from its increased human-computer interaction capability via eye tracking. The design principles and envisioned applications of the HRI-HMD are described, and the feasibility of the HRI-HMD is demonstrated by designing a prototype model.

1. Introduction

The field of Virtual Reality (VR) has recently received considerable attention, due to the potential to create unique capabilities for human-computer interaction [13, 15]. Such advanced interaction can include: interactive control and diagnostics systems, educational and training systems, teleoperation systems, and entertainment systems [5, 7, 11, 12, 17, 22]. For these applications, HMDs are typically used to provide visual information to the user [6]; however, conventional HMDs usually do not utilize the full potential of VR technology. In particular, they do not provide enough resolution or field of view to give the user the realistic feeling of being immersed in the computer-simulated virtual environment, nor support integrated effective interaction capabilities combining head and eye tracking.

For some applications, the feeling of being immersed in the computer-simulated world is critical for properly performing the required task. To give the user the feeling of immersion, two features of the HMD must be met. First, the display must provide a field of view large enough to surround the entire view. Second, it must provide resolution high enough to render the fine detail of the image. Too narrow of a field of view causes the user to see the frame of the display and to have the sense of looking through a window. To remove this perhaps annoying window effect, the field of view must be at least 80 degrees [19, 25]. Too low of a resolution causes the user to see the individual pixels or raster scans of the display device and fine details of the image are lost. To match human visual acuity, the pixel size must be about 1 arc minute [8]. However, the human retina does not provide uniform visual acuity [21, 24]. The high visual acuity is only available at the fovea, a small area of about 5° in angular extent at the center of the retina. The visual acuity degrades rapidly as the distance from the fovea increases; at an angular distance of 5° from the center of the fovea, it is about a quarter of the highest acuity, and at an angular distance of 15°, it becomes only one seventh [8]. Therefore, the resolution does not have to be 1 arc minute over a large field.

For a fixed number of pixels in a display, these two features are contradictory. A large field of view leads to low resolution, and high resolution leads to a small field of view. Consequently, most HMDs do not provide these two features adequately. To overcome this dilemma, HMDs that combine a low-resolution, large-field background image with a high-resolution, small-field insert image have been developed [3, 23]. Because of the property of the human visual system to have high visual acuity only over a narrow region around the fovea, a small area of high-resolution insert can be superposed on a large field of low-resolution image to virtually create a large field of view with high resolution. In this case, the position of the insert is dynamically controlled by the gaze point.

The approach taken by these systems is to use large high-resolution displays or light valves to generate the high-resolution insert and to use optics combined with a bundle of optical fibers to transport the images to the eyes. These systems provide significant improvements over ordinary displays and are considered the best displays

0-8186-7084-3/95 $04.00 © 1995 IEEE

Proceedings of the Virtual Reality Annual International Symposium (VRAIS '95)
0-8186-7084-3/95 $10.00 © 1995 IEEE

available, in spite of the fact that they are very heavy and extremely expensive.

Thus, currently available HMDs are either low-cost low-performance or high-cost high-performance models. Our approach is to develop an hybrid type, a low-cost high-performance insert HMD system that uses fully optoelectronic components. The use of fixed optoelectronic components allows the whole system to be fabricated with fewer alignment errors, to be immune to mechanical failure and, in general, to be more tolerant to vibrations.

The interaction capability currently integrated to HMDs is typically limited to the use of head tracking to measure the position and orientation of the user's head and to generate scenery from the user's perspective [10]. The user can navigate through the virtual world and interact with its objects by using three-dimensional manual input devices. For some situations that require very fast response time or difficult coordinated skills, the interaction capability supported by such manual input devices becomes inadequate. For those cases, eye movement can be used in conjunction with manual input devices to provide effective fast and flexible interaction methods.

The basic concept of the High-Resolution Insert HMD (HRI-HMD) described in this paper is to optically duplicate the insert image and to select one copy by blocking the other copies. The selected copy of the insert image is then optically superposed on the background image. The insert image traces the gaze point, thus the user sees the whole field at high resolution. The whole system uses fixed optical components and ordinary display devices. The availability of such a low-cost high-performance HMD will significantly increase the potential of many virtual reality applications. In addition to the apparent advantage of having a large-field, high-resolution image, the HRI-HMD provides effective interaction methods through eye tracking. Thus, combined with appropriate computer software, the whole system will become an Active Vision HMD (AV-HMD) system that gives the user the feeling of being immersed in the virtual environment and provides effective gaze-point-oriented interaction methods.

2. Applications

The primary advantage of the HRI-HMD is its large field of view with the existence of a high-resolution insert at the user's gaze point. The user can observe dynamic scenery over a large field at high resolution. Updates in the image do not have to occur simultaneously at high resolution. The portion of the image near the gaze point may be updated quickly at high resolution. However, other portions of the image may be updated less frequently or at lower resolution to reduce both the computational load and transmission bandwidth. The HRI-HMD can potentially improve the performance of real-time applications that require generation of complex computer graphics images, decompression of hierarchically compressed images, or transmission of remotely sensed images. Another use of the insert is to superpose different kinds of images at the gaze point. X-ray, ultrasound, or infrared heat images may be superposed over the regular visual spectrum images. The HRI-HMD with its built-in insert capability becomes advantageous for those applications.

The additional advantage is its increased interaction capability. The use of eye tracking is not limited to finding the gaze point for positioning the insert. The eye can respond to stimulus much faster than the hands [16]. Thus, the eyes can be used for fast and effective input, selection, and control methods. Various interaction methods can be realized through the use of hand, body, and eye movements [2, 4, 20].

3. Sytem Description and Objective

The HRI-HMD described in this paper inserts a small area of the high-resolution image on a large field of the low-resolution image, as shown in Figure 1.

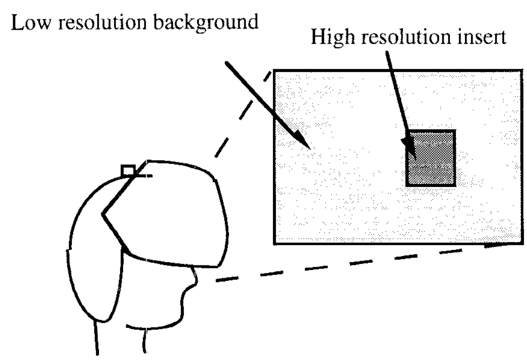

Figure 1. High-resolution insert HMD.

Using eye tracking information, the system dynamically places the high-resolution insert at the gaze point. Thus, in principle, the HRI-HMD visually provides the user with both high-resolution imagery and a large field of view. Several methods that may differ in accuracy can be used to track eye movements and the gaze points [1, 26]. The electro-oculography method detects the change of electric field in the tissue surrounding the eye and determines the orientation of the eye. This electric tracking method is the simplest method with moderate accuracy. The limbus tracking method detects the position of the limbus, which is the boundary between the iris and the sclera, and determines the gaze point. The pupil-corneal reflection method measures the corneal reflection with respect to the center of the pupil. These two optical tracking methods are much more accurate than the electric tracking method, however they require more complex hardware for

Proceedings of the Virtual Reality Annual International Symposium (VRAIS '95)
0-8186-7084-3/95 $10.00 © 1995 IEEE

processing. In order to determine the gaze point for superposing the high-resolution insert, the accuracy of the electro-oculography may be sufficient. To implement some of the complex human-computer interaction methods using the gaze point, the more accurate limbus tracking or pupil-corneal methods may be necessary. In either case, once the gaze point is determined, the superposition of the high-resolution insert over the low-resolution background is carried out using liquid crystal devices and fixed optical components. This will result in a low cost, reliable system. The schematic diagram of our HMD is shown in Figure 2.

There are two displays: one for the background and the other for the insert. The image of the insert display is optically duplicated to fill the entire background display, and a liquid crystal device array is used to select one element of the array. This means that only one copy of the insert display image passes through the liquid crystal array, and all the other copies are blocked. The images of the insert display and the background display are then combined using a beam splitter.

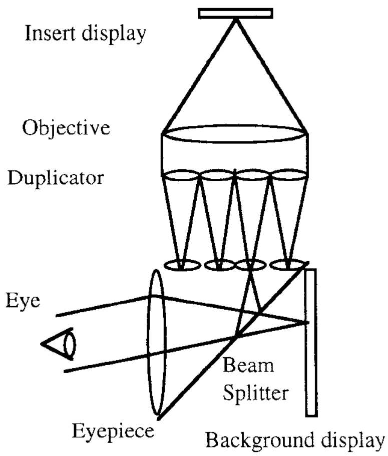

Figure 2. Schematic diagram of the HMD.

More specifically, the light from theinsert display is collimated by the objective. The collimated light is divided and focused by the duplicator to a set of identical images of the insert display, and the chief rays from these image points are set parallel to the optical axis. An array of liquid crystal shutters placed at the duplicator passes only one of these images and blocks the other images. These duplicated images are placed symmetrically to the background display with respect to the beam splitter so that the eye can see the superposed image through the eyepiece. The diagram represents the objective with a single lens, the duplicator with two arrays of lenses, and the eyepiece with another single lens.

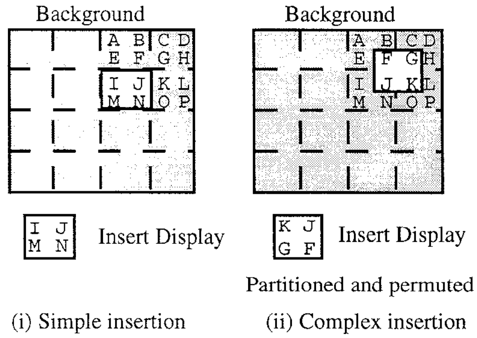

Figure 3. Superposition of the insert display.

The superposition of the insert and the background is depicted in Figure 3. In this figure, the shaded areas correspond to the background and the bright areas correspond to the insert. The character symbols represent contents of the image, and the dashed lines represent the cell boundary of the duplicated images. For a simple system, the insertion may be made at these discrete non-overlapping cell locations. In this case, the liquid crystal array may be placed anywhere inside the duplicator and blocks all the duplicated images except for one copy. When the insert image of "I J M N" is desired at a particular cell location, as shown in Figure 3-(i), this image can be directly displayed from the insert display. The duplicated images of "I J M N" fill every cell, and the copy of this image at that cell location exits the duplicator to be superposed with the background. For a complex system, the insertion may be made at continuous locations (up to the pixel level of the liquid crystal array). However, the size of the insert must be no larger than the size of a single duplicated image. In this case, the liquid crystal array must be placed near the duplicated image plane and blocks all the duplicated images except for some portions of up to four copies. When the insert image of "F G J K" is desired at a particular location, as shown in Figure 3-(ii), this image may be partitioned and permuted to "K J G F", and this transformed image can be displayed from the insert display. The duplicated images of "K J G F" fill every cell, and the portions of the four adjacent copies at that location which form the image of "F G J K" exit the duplicator to be superposed with the background.

The final goal of the design is to build a HMD that provides both a field of view large enough to surround the entire view and resolution high enough to match human visual acuity. The background must have a field of view of at least 80 degrees and resolution of 10 arc minutes, and the insert must have a field of view of at least 15 degrees and resolution of 1 arc minute. It must provide a stereoscopic view in color. The whole system must be integrated, folded, and packed in small volume so that the user can wear it without difficulty.

Proceedings of the Virtual Reality Annual International Symposium (VRAIS '95)
0-8186-7084-3/95 $10.00 © 1995 IEEE

4. Prototype Design

This prototype is a scaled-down version of the final model. First, the design parameters are determined from the constraints. To clarify the principles, an ideal thin-lens model of the system with the determined parameters is presented. Finally, a real model that was designed using an optical design tool, Zemax from Focusoft [14], is described.

4.1. Basic Configuration

The main component of the high-resolution insert is an optoelectronic system for duplicating the insert image and bringing the image to the eye. The basic configuration of this component can be organized in three stages, as shown in Figure 4.

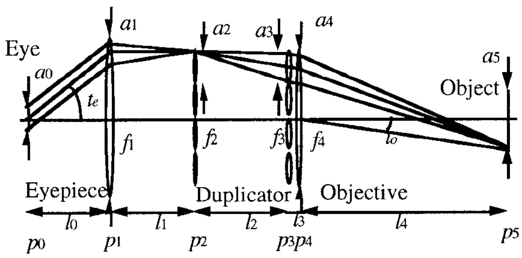

Figure 4. System parameters of the HMD.

The rightmost element is the insert display and the leftmost element is the eye. The first stage is the objective which collimates light from the display. The second stage is an array of telecentric systems which duplicate the display image from the collimated light and set the chief rays from the duplicated images parallel to the optical axis. We call this array of telecentric systems the duplicator. The third stage is the eyepiece which produces collimated light at the eye pupil from the duplicated image.

Miniature displays such as liquid crystal displays or viewfinders typically have 300 to 500 pixels in each direction. The largest field angle for an ordinary large field of view eyepiece is about 50 to 60 degrees. Thus, we arrive at the following basic design parameters:

	Background	Insert
Field	50°	12.5°
Pixels	400 x 400	400 x 400
Resolution	7.5 arc minutes 8 pixels/degree	1.875 arc minutes 32 pixels/degree

Table 1 : Basic design parameters

The distance between the eyepiece and its first focal plane where the duplicated images are located must be at least the physical size of the background display so that a beam splitter can be placed between the eyepiece and the duplicator to combine the insert and background images.

4.2. Ideal Thin-Lens Model

The ideal thin-lens model assumes ideal lenses of zero thickness. In other words, parallel beams to an ideal thin-lens with focal length f converge to a focal point at distance f from the lens. The height of the focal point from the optical axis is equal to $f \tan t$, where t is the angle that the parallel beams make with the optical axis.

In this ideal thin-lens model, $p_0, p_1, \ldots, p_5$ represent planes along the optical system, as shown in Figure 4. More specifically, the eye pupil resides at p_0 and the display object at p_5. The eyepiece uses a lens with focal length f_1 placed at p_1. The intermediate object at p_2 is viewed by the eye placed at p_0. The telecentric system used in the duplicator uses two lenses with focal lengths f_2 and f_3 placed at p_2 and p_3, respectively. Collimated beams at p_3 are imaged at p_2. The objective uses a lens with focal length f_4 placed at p_4. Beams from the display object at p_5 are collimated at p_4. The distance between planes p_i and p_{i+1} and the diameter of the aperture at p_i are denoted by l_i and a_i, respectively. The number of duplicated images along the vertical or horizontal axes is denoted by k. The largest chief ray angle at the eye pupil is t_e and the largest angle of the insert object subtended at the apex of the objective lens is t_o. These two parameters play essential roles in the ideal thin-lens model described.

The distances of both the eye and the duplicated images to the eyepiece lens must be equal to the focal length of the lens in order to obtain collimated beams at the eye pupil. Thus, we have

$$f_1 = l_0 = l_1 \quad . \tag{1}$$

Furthermore, the chief ray with the largest angle at the eye pupil is associated with the highest object point of the highest duplicated object. Thus, we have

$$l_0 \tan t_e = \frac{k\, a_2}{2} \quad . \tag{2}$$

For the telecentric system of the duplicator, collimated beams at p_3 must be focused at p_2, and beams passing the centers of the lenses at p_3 must exit parallel to the optical axis after passing p_2. Thus, we have

$$f_2 = f_3 = l_2 \quad . \tag{3}$$

Furthermore, the chief ray with the largest angle to the telecentric system at p_3 gives the highest image point for that element at p_2. Thus, we have

Proceedings of the Virtual Reality Annual International Symposium (VRAIS '95)
0-8186-7084-3/95 $10.00 © 1995 IEEE

$$l_2 \tan t_o = \frac{a_2}{2} \quad . \quad (4)$$

For the objective, the distance of the insert object to the lens must be equal to the focal length of the lens in order to obtain collimated beams from the object. Thus, we have

$$f_4 = l_4 \quad . \quad (5)$$

Furthermore, the ray with the largest angle subtended by the insert object at the lens apex is associated with the highest object point. Thus, we have

$$l_4 \tan t_o = \frac{a_5}{2} \quad . \quad (6)$$

Collimated beams at p_4 produce collimated beams at p_0. From this telescopic relationship, we have

$$\frac{a_0}{a_3} = \frac{l_1}{l_2} \quad . \quad (7)$$

From the relationship among the lens apertures, we get

$$a_1 > l_0 \tan t_e + \frac{a_0}{2} \quad , \quad (8)$$

$$a_4 > k\, a_2 \quad , \quad (9)$$

and

$$a_3 = c\, a_2 \quad \text{where } 0 < c \leq 1 \; . \quad (10)$$

The largest field angle of the eyepiece t_e and the number of duplicated images k can be calculated from the parameters given in Table 1. The exit pupil diameter a_0 must be at least 5 mm, but to allow some eye movements, a larger value is preferred. The insert display size a_5 may be about 25 mm for a typical miniature display. The ratio of the two lenses in the telecentric system, c, is ideally set close to 1.0 to maximize the brightness of the duplicated images, but physical constraints restrict it to be somewhat lower than this value. As the distance between the object and the objective lens decreases, the field angle of the objective increases, and so do field aberrations. Thus, a smaller field angle is preferred for minimizing aberration, but for compactness a larger angle is preferred. Thus, the largest field angle of the objective t_o may be limited to 6°. In summary, the following parameter values are assumed for the prototype:

$a_0 = 8$ mm, $a_5 = 25$ mm, $t_e = 25°$, $t_o = 6°$, $k = 4$, $c = 0.8$.

Solving the above equations, we determine the other parameter values as follows.

Combining Equations (1), (6), (7), and (10), the expression for f_1 is

$$f_1 = l_0 = l_1 = \frac{a_0}{2\, c \tan t_o} \quad . \quad (11)$$

From Equation (6), we have

$$l_4 = \frac{a_5}{2 \tan t_o} \quad . \quad (12)$$

Combining Equations (2) and (11), a_2 is given by

$$a_2 = \frac{a_0 \tan t_e}{k\, c \tan t_o} \quad . \quad (13)$$

Combining Equations (10) and (13), a_3 is given by

$$a_3 = \frac{a_0 \tan t_e}{k \tan t_o} \quad . \quad (14)$$

Finally, combining Equations (4) and (13), yields

$$f_2 = f_3 = l_2 = \frac{a_0 \tan t_e}{2\, k\, c \tan^2 t_o} \quad . \quad (15)$$

Table 2 lists the determined parameter values in millimeters:

i	a_i	f_i	l_i
0	8.000	-	47.572
1	52.366	47.572	47.572
2	11.092	52.765	52.765
3	8.873	52.765	1.000
4	44.368	118.930	118.930
5	25.000	-	-

Table 2 : Determined prototype parameters

The ideal thin-lens model layout at two different telecentric positions is shown in Figures 5-(i) and (ii).

4.3. Real Model

Since the purpose of designing a prototype is to show the feasibility of our approach, monochromatic light is assumed and our design is limited to the use of only spherical lenses of the same glass material (BK7). For more complete systems, chromatic aberration must be corrected by using different glass materials or more surfaces. Our design is further limited to the use of identical telecentrics in the duplicator.

Proceedings of the Virtual Reality Annual International Symposium (VRAIS '95)
0-8186-7084-3/95 $10.00

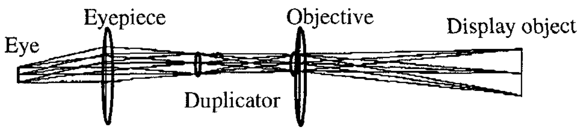

Figure 5-(i). Ideal thin-lens model layout at position 1.

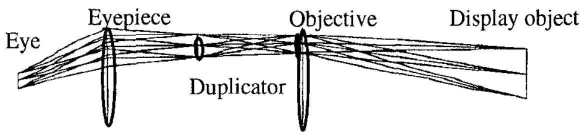

Figure 5-(ii). Ideal thin-lens model layout at position 2.

In this prototype design, the three stages are independently designed. The performance of the system may be improved by optimizing the system entirely by balancing aberrations from each stage.

The eyepiece uses four lenses and its layout is shown in Figure 6-(i). The object plane of the eyepiece, which symbolizes the duplicated images of the display formed by the objective and the duplicator, is the rightmost plane in Figure 6-(i). Light from this object is collimated and directed toward the eye pupil at the leftmost plane. The eye clearance is 15 mm. There is enough room for a beam splitter to be placed between the back lens surface and the focal plane. The performance of this eyepiece is shown in Figures 6-(ii) to (iv).

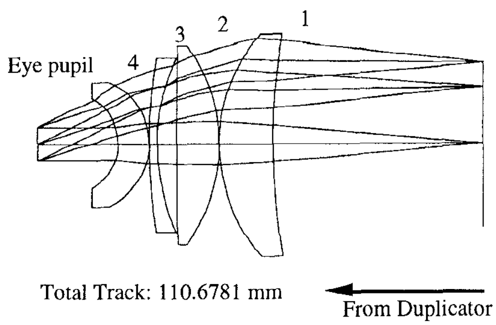

Figure 6-(i). Eyepiece layout.

The duplicator uses an array of telecentric systems. All the telecentric systems are identical and each uses four lenses. These lenses are imbedded in a square form. The layout of a single telecentric system is shown in Figure 7-(i). Collimated beams from the objective at the leftmost plane are focused at the rightmost plane. The rays passing the center of the first lens emerge parallel to the optical axis after passing the fourth lens. This guarantees that these rays, after passing the eyepiece, cross the optical axis at the eye pupil as shown in Figure 4. Thus, the first lens acts as an aperture and the fourth lens acts as a field stop. The performance of this telecentric system is shown in Figure 7-(ii).

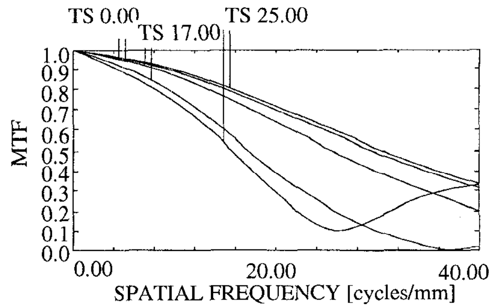

Figure 6-(ii) Eyepiece MTF.

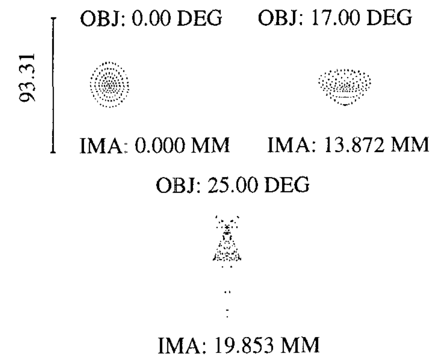

Field Degs :	0.00	17.00	25.00
RMS Radius :	11.03	12.64	14.35
GEO Radius :	15.54	21.20	46.65

Units are in microns

Figure 6-(iii) Eyepiece spot diagram.

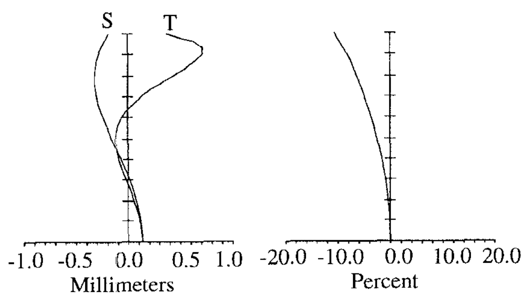

Figure 6-(iv) Eyepiece field curvature / distortion plot.

Proceedings of the Virtual Reality Annual International Symposium (VRAIS '95)
0-8186-7084-3/95 $10.00 © 1995 IEEE

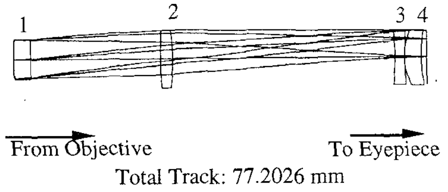

Figure 7-(i). Duplicator layout.

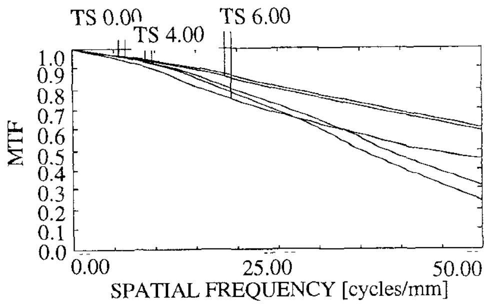

Figure 7-(ii). Duplicator MTF.

The objective uses four lenses and its layout is shown in Figure 8-(i).

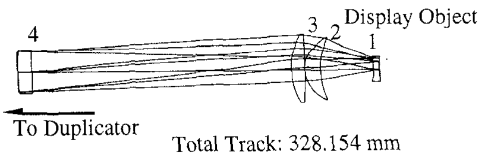

Figure 8-(i). Objective layout.

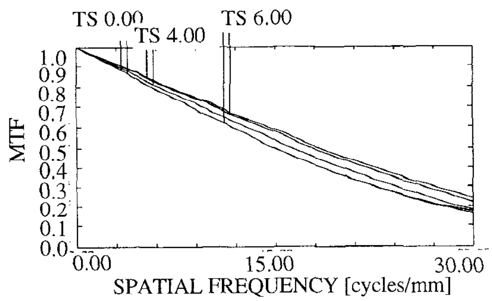

Figure 8-(ii). Objective MTF.

The display object is at the rightmost plane. Beams from this object are collimated at the leftmost plane. The performance of this objective is shown in Figure 8-(ii).

The layout of the entire system at two different telecentric positions is shown in Figures 9-(i) and 10-(i). For simplicity, the figures do not show the folding of the system nor combining the insert and the background. The folding and combining can be done between the eyepiece and the duplicator. Further folding can be made within the duplicator and the objective. The performance of the entire system at these two telecentric positions is shown in Figures 9-(ii) to (iv) and 10-(ii) to (iv).

Because of the symmetry of the system, the performance at positions 3 and 4 is equivalent to that of 1 and 2.

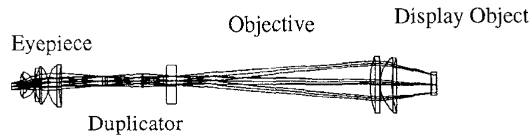

Figure 9-(i). Real model layout at position 1.

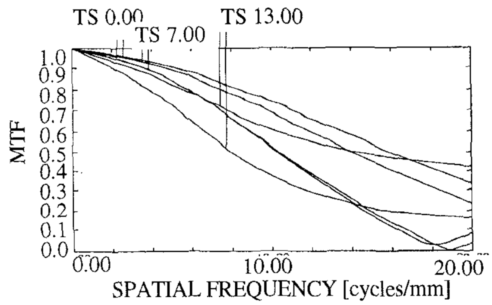

Figure 9-(ii). Real model MTF at position 1.

5. Discussion and Future Research

5.1. Prototype Performance

The insert image has 200 line-pairs in each direction. The size of this insert image at the insert display plane at p_5 is 25 mm, which results in a spatial frequency of 8 lp/mm. At the duplicated image plane at p_2, the size of this insert image is 11.092 mm, which results in a spatial frequency of 18 lp/mm. Each stage as well as the entire system are analyzed from their collimated object planes to their focused image planes. For the eyepiece, its focused image plane is at p_2, and thus the required spatial frequency is 18 lp/mm. For the telecentric system in the duplicator, the required spatial frequency is also 18 lp/mm, since its focused image plane is also at p_2. For the objective, its focused image plane is at p_5, and thus the required spatial frequency is 8 lp/mm. For the entire system, the required

Proceedings of the Virtual Reality Annual International Symposium (VRAIS '95)
0-8186-7084-3/95 $10.00 © 1995 IEEE

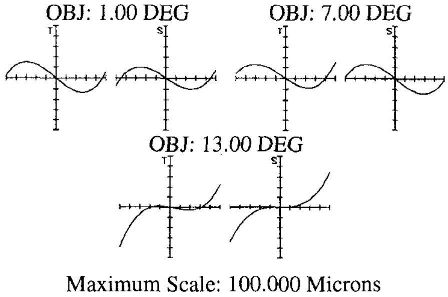

Figure 9-(iii) Real model rayfan plot at position 1.

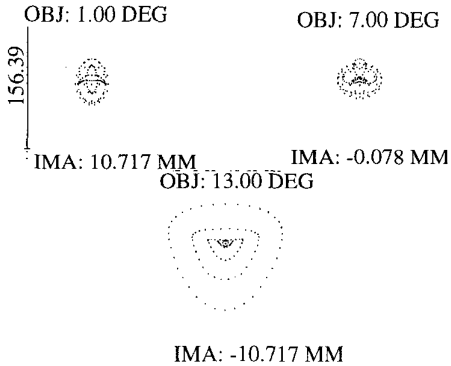

Field Degs:	1.00	7.00	13.00
RMS Radius	17.62	19.37	40.44
GEO Radius:	29.75	30.92	78.19

Units are in microns

Figure 9-(iv) Real model spot diagram at position 1.

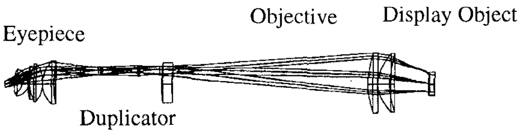

Figure 10-(i). Real model layout at position 2.

spatial frequency is also 8 lp/mm, since its focused image plane is also at p_5. If there is no balancing of aberrations from different stages, the MTF of the entire system is the product of the MTF of each stage. Thus, to get a MTF of 0.5 for the entire system at this required spatial frequency, the MTF of each stage at this spatial frequency must be at least 0.8. The MTFs of the duplicator and the objective

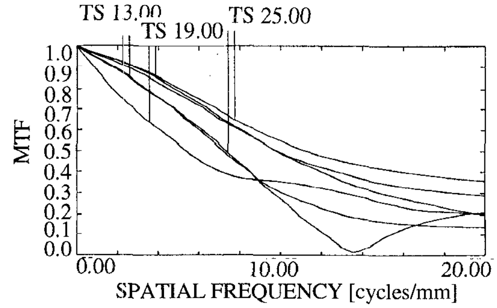

Figure 10-(ii). Real model MTF at position 2.

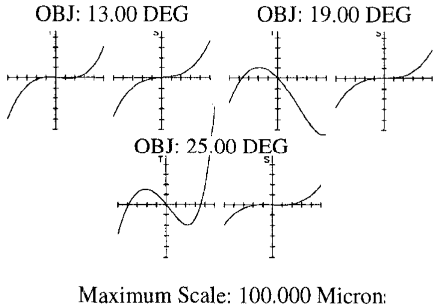

Figure 10-(iii). Real model rayfan plot at position 2.

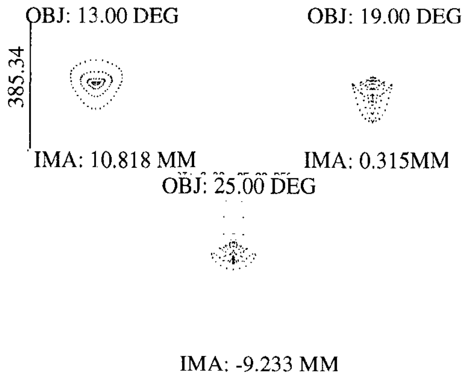

Field Degs:	13.00	19.00	25.00
RMS Radius:	44.83	51.72	50.03
GEO Radius:	79.08	108.66	192.67

Units are in microns

Figure 10-(iv). Real model spot diagram at position 2.

show that the system is capable of resolving this limit. The eyepiece is limited by astigmatism which limits the performance of the entire system at large angles. For the entire system, the required spatial frequency is 8 lp/mm. The MTFs of the entire system show that they are capable of resolving the required spatial frequency.

Proceedings of the Virtual Reality Annual International Symposium (VRAIS '95)
0-8186-7084-3/95 $10.00

The limitations of the entire system currently comes from mainly the coma, astigmatism, and field curvature of each stage. Between the objective and the duplicator, these aberrations can be balanced, since they form a point-to-point imaging system as a pair. The astigmatism and field curvature of the eyepiece may be reduced by using telecentric systems with different focal lengths or displacements to bend the object plane of the eyepiece. In our prototype, the duplicator uses lenses at the image plane (the object plane for the eyepiece) to align the principal rays parallel to the optical axis. This may introduce a practical problem, since any scratches or dusts on these lenses significantly degrade the image quality. To avoid this problem, these lenses may be placed away from the image plane as long as the collimated beams reach the pupil of the eye.

5.2. Future Systems

Our prototype design is the first step to a more complete HMD system that can be used in the described applications. Extensions to our prototype design include:

Use of a color display,
Use of a display with more pixels,
Use of non spherical surfaces or binary optics,
Integration with an eye tracker,
Fabrication and packaging,
System demonstration for the described applications.

To use a color display, chromatic aberration must be corrected using glasses with different refractive indices. The resolution and field of view can be increased by using a display with more pixels as long as the optical system supports its spatial frequency.

For a higher performance at the expense of more complex structures, non spherical lenses or binary optical elements may be used to optimize the system. Such complex surfaces are particularly suited for the eyepiece, since each small portion of the angular area can be independently optimized. The eyepiece also serves for the background, however the quality of the background image is not critical. Therefore, the eyepiece can be tuned for the insert image.

As mentioned earlier, the ordinary eyepieces have their field of view limited to about 60°. To obtain a larger field of view, eyepieces with intentionally distorted imaging properties may be used [18]. In this case, both the background and insert images for the HRI-HMD have to be predistorted so that the correct imagery can be viewed by the user.

Even if such an intentionally distorted eyepiece is assumed, in order to keep enough room between the eyepiece and its image plane for folding, a significant tradeoff between the image quality and the field of view may remain. In this case, the image quality of both the background and insert at a larger angle may be sacrificed for some extent to maintain the large field of view. A relatively high image quality may be retained for the insert by optimizing each angular section of the eyepiece.

All components including the eye tracker must be integrated and fabricated as an HMD.

Finally, the system performance for the described applications must be demonstrated. A set of software tools has to be developed to utilize the functionality of the HMD.

6. Conclusion

We introduced a new high-resolution insert HMD, named the High-Resolution Insert HMD (HRI-HMD), and designed its first prototype model. The HRI-HMD uses only optoelectronic devices and no mechanical devices. The apparent benefit of the HRI-HMD is its potential for providing a large-field, high-resolution image. The additional benefit is its potential for supporting various gaze point oriented interaction methods. We presented its principles by formalizing the system design parameters, and demonstrated its feasibility by presenting the design of a prototype system. We also described potential applications of the HRI-HMD systems.

Acknowledgements

The authors thank Prof. Gerhard Schlimbach and Mr. Claus Neubronner at the FH Rheinland-Pfalz, Worms, Germany for their kind support by allowing the use of their equipment.

References

1. Applied Science Laboratories, Eye tracking systems handbook, (Applied Science Laboratories, Waltham, MA, 1992).

2. R. A. Bolt, "Gaze-orchestrated dynamic windows," Computer Graphics, 15(3), 109-119 (1981).

3. D. Burbidge and P. M. Murray, "Hardware improvement to the helmet mounted projector on the visual display research tool (VDRT) at the Naval Training Systems Center," Proc. SPIE Vol. 1116, 52-60 (1989).

4. S. Bryson, "Interaction of objects in a virtual environment: a two-point paradigm," Proc. SPIE Vol. 1457, 180-187 (1991).

5. G. Burdea and P. Coiffet, Virtual Reality Technology, (Wiley & Sons, New york, NY, 1994).

6. J. C. Chung, M. R. Harris, F. P. Brooks, H. Fuchs, M.T. Kelley, J. Hughes, M. Ouh-young, C. Cheung, R. L. Holloway, and M. Pique, "Exploring virtual worlds with

Proceedings of the Virtual Reality Annual International Symposium (VRAIS '95)
0-8186-7084-3/95 $10.00 © 1995 IEEE

head-mounted displays," Proc. SPIE Vol. 1083, 42-52 (1989).

7. R. E. Cole, C. Ikehara, and J. O. Merritt, "A low cost helmet-mounted camera/display system for field testing teleoperator tasks," Proc. SPIE Vol. 1669, 228-235 (1992).

8. H. Davson, Physiology of the eye, 5th ed. (Pergamon Press, New York, 1990).

9. S. Feiner, S. Nagy, and A. van Dam, "An experimental system for creating and presenting interactive graphical document," ACM Trans. Graphics 1(1), 59-77 (1982).

10. F. J. Ferrin, "Survey of helmet tracking technologies," Proc. SPIE Vol. 1456, 86-94 (1991).

11. S. S. Fisher, M. McGreevy, J. Humphries, and W. Robinett, "Virtual environment display system," ACM Workshop on Interactive 3D Graphics, Oct 23-24, Chapel Hill, North Carolina (1986).

12. S. S. Fisher, M. W. McGreevy, J. Humphries, and W. Robinett "Virtual interface environment for telepresence applications," in Proceedings of the ANS International Topical Meeting on Remote Systems and Robotics in Hostile Environments, J. D. Berger, ed. (1987).

13. S. S. Fisher, "Virtual interface environments," in The Art of Human-Computer Interface Design, B. Laurel ed. (Addison-Wesley, Menlo Park, CA, 1990), pp.423-438.

14. Focusoft, Zemax optical design program user's guide ver. 3.0, (Pleasanton, California 94566, 1994).

15. D. Foley, "Interfaces for Advanced Computing," Scientific American 257(4), 126-135 (1987).

16. H. Girolamo, "Notional helmet concepts: A survey of near-term and future technologies," US Army NATICK Technical Report NATIK/TR-91/017 (1991).

17. C. Herot, "Spatial management of data," ACM Trans. Database Systems 5(4), 493-514 (1980).

18. E. M. Howlett, "Wide angle orthostereo," Proc. SPIE Vol. 1256, 210-223 (1990).

19. E. M. Howlett, "High-resolution inserts in wide-angle head-mounted stereoscopic displays," Proc. SPIE Vol. 1669, 193-203 (1992).

20. R. H. Jacoby and S. R. Ellis, "Using virtual menus in a virtual environment," Proc. SPIE Vol. 1668, 39-47 (1992).

21. R. A. Moses, Adlers Physiology of the eye, The C.V. Mosby Company (1970).

22. D. Thalmann, Using virtual reality techniques in the animation process, in Virtual Reality Systems, R. A. Earnshaw, M. A. Gigante, and H. Jones ed. (Academic Press, Reading, MA, 1993).

23. M. L. Thomas, W. P. Siegmund, S. E. Antos, and R. N. Robinson, "Fiber optic development for use on the fiber optic helmet mounted display," Proc. SPIE Vol. 1116, 90-101 (1989).

24. G. Westheimer, The eye as an optical instrument, in Hanbook of Perception and Human Performance Vol I., 4 (Wiley-Interscience, New York, NY, 1986).

25. H. Yamaguchi, A. Tomono, and Y, Kobayashi, "Proposal for a large visual field display employing eye movement tracking," Proc. SPIE Vol. 1194, 13-20 (1989).

26. L. Young and D. Sheena, "Survey of eye movement recording methods," Behavior Research Methods, Instruments and Computers Vol. 7, 397-429 (1975).

Proceedings of the Virtual Reality Annual International Symposium (VRAIS '95)
0-8186-7084-3/95 $10.00 © 1995 IEEE